

Effect of Magnetic Anisotropy Constants on Skyrmion Formation in Co/Pt

Tamali Mukherjee, V Satya Narayana Murthy@

Department of Physics, BITS Pilani Hyderabad Campus, Telangana, India

@satyam@hyderabad.bits-pilani.ac.in

Abstract

Skyrmions, which are topologically stable magnetic structures, have manifested promising features to be used as an information carrier in new-age, non-volatile data storage devices. In this article, we show how the creation and stability of skyrmion can be manipulated by external stimuli (here, nano-second current pulse). Co/Pt square nano-structure with Co free layer thickness in the range 1 nm to 5 nm and first and second-order anisotropy constants are taken to study the controlled creation of skyrmions. The magnetization dynamics controlled by the current-induced spin transfer torque help to nucleate skyrmions by transformation from perpendicularly magnetized ground state to a stable state of isolated skyrmions via complex transformation of Neel wall following its image inversion. Compared with the first-order anisotropy alone, how the higher-order anisotropy constants (up to second order) impact the relaxed state of a system has been discussed.

Keywords: Skyrmions, Dzyaloshinskii-Moriya interaction, Magnetic nano-structures, Spintronics, Magnetic anisotropy.

Introduction

Since 1989, various theoretical studies have shown that an asymmetric exchange interaction called Dzyaloshinskii-Moriya Interaction (DMI) [1, 2] can stabilize isolated magnetic vortices. Magnetic skyrmions are small (a few nanometers to several microns), swirling, vortex-like structures in magnetic materials that arise due to competing effects from Heisenberg exchange interaction and DMI [3 - 5]. They are uniquely characterized by topological charge ± 1 [4 - 7].

$$Q = \frac{1}{4\pi} \int dx \int dy \left(\frac{\partial \vec{m}}{\partial x} \times \frac{\partial \vec{m}}{\partial y} \right) \cdot \vec{m} \text{ --- (1)}$$

Magnetic skyrmions have been observed in bulk and thin film magnetic materials with broken inversion symmetry [3, 5, 8]. The interfacial DMI between heavy metal (HM) / ferromagnetic (FM) layers such as Pt/Fe, Pd/Co, Ni/Co, and Pt/CoFeB helps in stabilizing skyrmions [5,9]. The stabilization of skyrmion depends on the DMI constant [10] determined by the thickness of the heavy metal and the properties of the HM/FM interface [11, 12]. Co or CoFeB based

multilayer stacks tend to exhibit larger DMI, and that makes them significant in the context of stabilization of skyrmions [13-15]. Also, the effective strength of DMI depends on the thickness of the ferromagnetic layer. The higher the thickness of the ferromagnetic layer, the less DMI will be effective [8].

$$D_{eff} = \frac{D}{t_{FM}} \text{---} \text{---} \text{---} \text{---} \text{---} (2)$$

Where, D_{eff} is the effective DMI strength, D is the interfacial DMI, and t_{FM} is the thickness of the ferromagnetic layer.

Along with DMI, magnetic anisotropy energy also plays a vital role in nucleating and holding skyrmion in the system. The anisotropy constant balances the force in the material, and by preventing the magnetic moments from easily flipping to a random direction, it secures the skyrmion to exist in the material. The stabilization of skyrmion largely depends on the anisotropy energy as it controls the total energy landscape of the material [16,17].

Magnetic skyrmions show promising features to be used as an information carrier for new age non-volatile memory devices due to their small size and low energy cost to manipulate them. Easy creation and deletion are essential in the context of practical usage of skyrmions [18 - 22]. Despite isolated skyrmions and lattices of skyrmions already being observed in experiments, the controlled creation still needs to be explored. In this article, we show, how a current can affect the states of a perpendicularly magnetized square nano-structure by Spin Transfer Torque (STT) by considering the first and second-order anisotropy constants. A stable state of isolated skyrmions is nucleated in Co/Pt multilayers by optimizing the current density.

Material & Method

The square nano-structures we consider here are FM/HM layers of Co/Pt (Fig. 1). The free layer Co has dimensions 200 nm x 200 nm and varied thicknesses from 1 nm to 5 nm. The non-magnetic spacer layer (Pt) separates the free layer from the ferromagnetic fixed layer. The free layer is in the x-y plane and has perpendicular magnetization along the +z direction. The fixed layer magnetization m_p is along the +x direction (1,0,0).

GPU-accelerated micromagnetic software Mumax3 [23] solves the Landau-Lifshitz-Gilbert equation (LLG) using a finite difference approach. Cuboid cells of dimensions 1 nm x 1 nm x

1 nm are used, and the temperature is set at zero to avoid thermal fluctuations. The change in magnetization (m) of the free layer Co with time (t) is governed by the LLG equation [24, 25],

$$\frac{\partial \vec{m}}{\partial t} = -\gamma (\vec{m} \times \vec{H}_{eff}) + \alpha \left(\vec{m} \times \frac{\partial \vec{m}}{\partial t} \right) + \vec{I}_{STT} \quad (3)$$

Here, γ and α are the gyromagnetic ratio and Gilbert damping constant, respectively. The effective field (H_{eff}) [26] is $H_{eff} = H_{ex} + H_{anis} + H_{dip} + H_{DMI} + H_0$, respectively stands for exchange field, magnetocrystalline anisotropy field, dipolar field, DMI field, and the Oersted field provided by the applied current.

Spin Transfer Torque (\vec{I}_{STT}) is given by,

$$\vec{I}_{STT} = \gamma a (\vec{m} \times (\vec{m}_p \times \vec{m})) - \gamma b (\vec{m} \times \vec{m}_p) \quad (4)$$

where,

$$a = \frac{\hbar J}{2t_{Co} e M_s} \frac{p \Lambda^2}{(\Lambda^2 + 1) + (\Lambda^2 - 1)(\vec{m} \cdot \vec{m}_p)} \quad (5)$$

$$\text{and, } b = \frac{\hbar J \epsilon}{2t_{Co} e M_s} \quad (6)$$

here, \hbar = Planck's constant, J = current density, t_{Co} = thickness of cobalt free layer, e = electronic charge, M_s = saturation magnetization, p = conduction electron polarization, ϵ = coefficient of field-like torque and for the present study, we have used $p = 0.5$, $\Lambda = 1.0$, and $\epsilon = 0$.

The material parameters essential for the simulation used are, saturation magnetization (M_s) = 5.80×10^5 A/m, exchange constant (A_{ex}) = 1.5×10^{-11} J/m, DMI constant (D_{int}) = 3×10^{-3} J/m², Gilbert damping parameter (α) = 0.1, and anisotropy constants (K_{u1} & K_{u2}) = 6×10^5 J/m³ & 1.5×10^5 J/m³ are taken to stabilize easy-cone state [27 - 29]. Furthermore, keeping all the other parameters same, instead of taking first and second-order magnetic anisotropy constants, we considered perpendicular magnetic anisotropy (PMA) constant $K_{u1} = 8 \times 10^5$ J/m³ to study how the anisotropy constants affect the final ground state spin configuration of the system.

Results and Discussions

At $t = 0$ sec, all the spins in the free layer are perpendicular to the sample plane (+z direction). The fixed layer magnetization m_p is along (1,0,0) direction. Current density of magnitude 2×10^{12} A/m² – 10×10^{12} is applied for 0.5 ns and then reversed for 0.07 ns to 0.1 ns. For $t_{Co} = 1$ nm and $J = 1 \times 10^{12}$ A/m² the ground state of the system remains unchanged. Further, the

excitation current increased to $J = 2 \times 10^{12} \text{ A/m}^2$, applied in the $+z$ direction for 0.5 ns, the spin configuration of the perpendicularly magnetized free layer (Fig. 2(a)) changes to in-plane and forms a Neel wall (Fig. 2(b)). Then, the Neel wall goes through its image inversion (Fig. 2(c)) for the reversed current density of the same magnitude, applied for 0.1 ns. The final ground state of the system (Fig. 2(e)) is a 180° domain wall separating two reversely magnetized domains.

Then, we increased the current pulse density (J) to $2.3 \times 10^{12} \text{ A/m}^2$ and applied for 0.5 ns in $+z$ direction and in $-z$ -direction for 0.07 ns. Just before the current pulse is applied (in the relaxed state), all the spins are perpendicularly aligned to the plane of the system, as shown in Fig. 3(a). The domain wall started to form (Fig. 3(b)) at $t = 0.5$ ns. From Fig. 3(c) (at 0.57 ns), it is evident that, by reversing the current density, the Neel wall starts transforming into its image inversion. In the absence of any applied current, a state of four isolated skyrmions of opposite core magnetization starts appearing at 0.8 ns (Fig. 3(e)) following a complicated transformation (Fig. 3(d)) at the intermediate time. Finally, from $t = 3.75$ ns onwards, the four skyrmions got stable at their positions along with the presence of a 180° domain wall (Fig. 3(g)). The calculated diameters of the nucleated skyrmions range between 10 nm to 13 nm.

Fig. 3(h), shows the topological charge (Q) variation of $t_{co} = 1$ nm. During the time when the current from $+z$ direction flipped into the $-z$ direction, Q is found to be - 3.23 (at $t = 0.55$ ns). Then, after switching off the current at 0.57 ns, Q changes to 1.48 at $t = 0.61$ ns. Throughout the simulation time from $t = 0.5$ ns to $t = 0.9$ ns, the system undergoes complicated domain transformation triggered by the mechanism of magnetization reversal induced by STT provided by the applied current. The simulation calculates the overall Q of the sample, the graph shows the rapid fluctuation of topological charge during the time mentioned earlier. From $t = 0.9$ ns onwards, the topological charge of the system becomes zero as it relaxes to a stable state of four skyrmions, with two having $Q = +1$ and the other two having $Q = -1$.

From fig. 4(a), the STT provided by the applied current density (J) = $2.3 \times 10^{12} \text{ A/m}^2$ is higher than $J = 2 \times 10^{12} \text{ A/m}^2$. Following that in fig. 4(b), we can see the total energy (E_{total}), and exchange and DMI energy ($E_{Exchange + DMI}$) variation. For $J = 2.3 \times 10^{12} \text{ A/m}^2$, the combination of DMI energy (E_{DMI}) and exchange energy ($E_{Exchange}$) becomes higher and makes the total energy (E_{total}) also higher. As a result, the system relaxes to a stable skyrmion state along with

a 180° domain wall (fig. 4(c)). The system relaxes to a stable state with a 180° domain wall (fig. 2(e)) for the current density (J) = 2×10^{12} A/m².

With the increase in thickness, the current density required to nucleate and hold skyrmions in the nano-structure is higher. Keeping the current pulse widths same as in the case of $t_{Co} = 1$ nm, for $t_{Co} = 2$ nm, no skyrmion is observed. Then, we increase the current density (J) = 5×10^{12} A/m² and apply it in the +z direction for 0.5 ns and in the -z direction for 0.08 ns three skyrmions get nucleated (Fig. 5(a)). For, positive pulse width (in +z direction) of 0.5 ns and negative pulse width (in -z direction) of 0.1 ns the threshold current density to nucleate skyrmion is 7×10^{12} A/m² for 3 nm (Fig. 5(b)), 8×10^{12} A/m² for 4 nm (Fig. 5(c)), and 10×10^{12} A/m² for 5 nm (Fig. 5(d)).

Moreover, for $t_{Co} = 5$ nm, we apply a current density $J = 10 \times 10^{12}$ A/m² in +z direction for 0.5 ns and in -z direction for 0.08 ns. Fig. 6(a) shows 3 skyrmions of the same core magnetization generated in a single domain, and no domain wall is observed. It clarifies how the minute change in negative pulse width also affects the final ground state of the system. Also, this concludes that, with the manipulation of applied current density, the number of nucleated skyrmions can be controlled.

In the above study, instead of considering only the first-order magnetic anisotropy constant, which provides the conventional perpendicular magnetic anisotropy (PMA) [26, 30, 31], we have taken easy-cone state configuration by taking both first and second-order magnetic anisotropy constants (values are mentioned in 'Material and Methods' section). From fig. 7(b), we can see that for $t_{Co} = 1$ nm, and current density $J = 2.3 \times 10^{12}$ A/m² applied in +z direction for 0.5 ns and in -z direction for 0.07 ns and only considering first order anisotropy constant (K_{u1}), the relaxed state will be only a domain wall. However, by taking first and second order, both the anisotropy constants into consideration, the system relaxes to a stable state of 4 skyrmions along with a domain wall (Fig. 3(g)). It confirms that the magnetic anisotropy energy plays a crucial role in the stabilization of skyrmion, and the final relaxed spin state configuration in both cases are not the same even after applying the current of the same magnitude with identical positive and negative pulse widths.

Conclusions

The controlled creation of skyrmions with nano-second current pulses in a square Co/Pt nano-structure, with Co thicknesses range of 1 – 5 nm, is studied by employing micromagnetic simulation via Mumax3. A maximum number of 4 skyrmions is observed, for current densities ranging between 2×10^{12} A/m² to 10×10^{12} A/m² applied in +z direction for 0.5 ns and in -z direction for 0.07 ns to 0.1 ns (modulated in steps of 0.005 ns). A slight change in the negative pulse width causes a significant change in the relaxed state because of the complicated transformation of the spin system during this time. To understand the role of magnetic anisotropy in stabilizing skyrmions, cone anisotropy (first-order + second-order anisotropy constants) and first-order constant alone are used in the study. Simulating skyrmions in the nano-structure is energetically more favourable when first and second-order anisotropy constants are considered.

Acknowledgments

We acknowledge BITS Pilani Hyderabad Campus for providing the Sharanga High-Performance Computational facility to carry the above work.

References

- [1] Bogdanov, Alexei N., and D. A. Yablonskii, "Thermodynamically stable “vortices” in magnetically ordered crystals. The mixed state of magnets." *Zh. Eksp. Teor. Fiz* 95.1 (1989): 178. <https://jetp.ras.ru/cgi-bin/e/index/e/68/1/p101?a=list>
- [2] Dzyaloshinsky, Igor, "A thermodynamic theory of “weak” ferromagnetism of antiferromagnetics." *J. Phys. Chem. Solids* 4.4 (1958): 241-255. [https://doi.org/10.1016/0022-3697\(58\)90076-3](https://doi.org/10.1016/0022-3697(58)90076-3)
- [3] Tokura, Yoshinori, and Naoya Kanazawa, "Magnetic skyrmion materials." *Chem. Rev.* 121.5 (2020): 2857-2897. <https://doi.org/10.1021/acs.chemrev.0c00297>
- [4] Roessler, Ulrich K., A. N. Bogdanov, and C. Pfleiderer, "Spontaneous skyrmion ground states in magnetic metals." *Nature* 442.7104 (2006): 797-801. <https://doi.org/10.1038/nature05056>
- [5] Dohi, Takaaki, Robert M. Reeve, and Mathias Kläui, "Thin film skyrmionics." , *Annu. Rev. Condens. Matter Phys.* 13 (2022): 73-95. <https://doi.org/10.1146/annurev-conmatphys-031620-110344>

- [6] Manton, Nicholas, and Paul Sutcliffe, *Topological solitons*, Cambridge University Press, 2004.
- [7] Thiaville, André, Jacques Miltat, and Stanislas Rohart, "Magnetism and topology." in : *Magnetic Skyrmions and Their Applications*. Woodhead Publishing, 2021. 1-30. <https://doi.org/10.1016/B978-0-12-820815-1.00012-2>
- [8] Litzius, Kai, and Mathias Kläui, "Materials for skyrmionics." in : *Magnetic Skyrmions and Their Applications*. Woodhead Publishing, 2021. 31-54. <https://doi.org/10.1016/B978-0-12-820815-1.00001-8>
- [9] Wang Kang, Yangqi Huang, Xichao Zhang, Yan Zhou and Weisheng Zhao, "Skyrmion-electronics: An overview and outlook." *Proceedings of the IEEE* 104.10 (2016): 2040-2061. <https://doi.org/10.1109/JPROC.2016.2591578>
- [10] Rohart, S., and A. Thiaville. "Skyrmion confinement in ultrathin film nanostructures in the presence of Dzyaloshinskii-Moriya interaction." *Phys. Rev. B* 88.18 (2013): 184422. <https://doi.org/10.1103/PhysRevB.88.184422>
- [11] Mohamed Belmeguenai, Jean-Paul Adam, Yves Roussigné, Sylvain Eimer, Thibaut Devolder, Joo-Von Kim, Salim Mourad Cherif, Andrey Stashkevich, and André Thiaville, "Interfacial Dzyaloshinskii-Moriya interaction in perpendicularly magnetized Pt/Co/AlO_x ultrathin films measured by Brillouin light spectroscopy.", *Phys. Rev. B* 91.18 (2015): 180405. <https://doi.org/10.1103/PhysRevB.91.180405>
- [12] Y. Quessab, J-W. Xu, C. T. Ma, W. Zhou, G.A. Riley, J. M. Shaw, H. T. Nembach, S. J. Poon and A. D. Kent, "Tuning interfacial Dzyaloshinskii-Moriya interactions in thin amorphous ferrimagnetic alloys." , *Sci. Rep.* 10.1 (2020): 7447. <https://doi.org/10.1038/s41598-020-64427-0>
- [13] Runze Chen, Xinran Wang, Houyi Cheng, Kyu-Joon Lee, Danrong Xiong, Jun-Young Kim, Sai Li, Hongxin Yang, Hongchao Zhang, Kaihua Cao, Mathias Kläui, Shouzhong Peng, Xueying Zhang and Weisheng Zhao, "Large Dzyaloshinskii-Moriya interaction and room-temperature nanoscale skyrmions in CoFeB/MgO heterostructures." *Cell Rep. Phys. Sci.* 2.11 (2021). <https://doi.org/10.1016/j.xcrp.2021.100618>
- [14] Fakhredine, Amar, Andrzej Wawro, and Carmine Autieri, "Huge Dzyaloshinskii-Moriya interactions in Re_Co_Pt thin films." *arXiv preprint arXiv:2310.03638* (2023). <https://doi.org/10.48550/arXiv.2310.03638>
- [15] Mirko Baćani, Miguel A. Marioni, Johannes Schwenk & Hans J. Hug "How to measure the local Dzyaloshinskii-Moriya interaction in skyrmion thin-film multilayers." *Sci. Rep.* 9.1 (2019): 3114. <https://doi.org/10.1038/s41598-019-39501-x>
- [16] M. N. Wilson, A. B. Butenko, A. N. Bogdanov, and T. L. Monchesky, "Chiral skyrmions in cubic helimagnet films: The role of uniaxial anisotropy." *Phys. Rev. B* 89.9 (2014): 094411. <https://doi.org/10.1103/PhysRevB.89.094411>

- [17] Dieny, B., and M. Chshiev. "Perpendicular magnetic anisotropy at transition metal/oxide interfaces and applications." *Rev. Mod. Phys.* 89.2 (2017): 025008.
<https://doi.org/10.1103/RevModPhys.89.025008>
- [18] Fert, Albert, Nicolas Reyren, and Vincent Cros, "Magnetic skyrmions: advances in physics and potential applications." *Nat. Rev. Mater.* 2.7 (2017): 1-15.
<https://doi.org/10.1038/natrevmats.2017.31>
- [19] Finocchio, Giovanni, Felix Büttner, Riccardo Tomasello, Mario Carpentieri and Mathias Kläui, "Magnetic skyrmions: from fundamental to applications." *J. Phys. D: Appl. Phys.* 49.42 (2016): 423001. <http://dx.doi.org/10.1088/0022-3727/49/42/423001>
- [20] Ralph, Daniel C., and Mark D. Stiles, "Spin transfer torques.", *J. Magn. Magn. Mater.*, 320.7 (2008): 1190-1216. <https://doi.org/10.1016/j.jmmm.2007.12.019>
- [21] Fert, Albert, Vincent Cros, and Joao Sampaio. "Skyrmions on the track." *Nat. Nanotechnol* 8.3 (2013): 152-156. <https://doi.org/10.1038/nnano.2013.29>
- [22] Wang, Kang, et al. "Fundamental physics and applications of skyrmions: A review." *J. Magn. Magn. Mater.* (2022): 169905.
<https://doi.org/10.1016/j.jmmm.2022.169905>
- [23] Arne Vansteenkiste, Jonathan Leliaert, Mykola Dvornik, Mathias Helsen, Felipe Garcia-Sanchez and Bartel Van Waeyenberge, "The design and verification of MuMax3." *AIP Adv.* 4.10 (2014). <https://doi.org/10.1063/1.4899186>
- [24] Lakshmanan, M, "The fascinating world of the Landau–Lifshitz–Gilbert equation: an overview." *Philos. Trans. Royal Soc.* A369.1939 (2011): 1280-1300.
<https://doi.org/10.1098/rsta.2010.0319>
- [25] Kumar, D., and A. O. Adeyeye, "Techniques in micromagnetic simulation and analysis." *J. Phys. D: Appl. Phys* 50.34 (2017): 343001. <https://doi.org/10.1088/1361-6463/aa7c04>
- [26] Yuan, H. Y., and X. R. Wang, "Skyrmion creation and manipulation by nano-second current pulses." *Sci. Rep.* 6.1 (2016): 22638. <https://doi.org/10.1038/srep22638>.
- [27] Maverick Chauwin , Xuan Hu , Felipe Garcia-Sanchez , Neilesh Betrabet, Alexandru Paler, Christoforos Moutafis and Joseph S. Friedman , "Skyrmion logic system for large-scale reversible computation." *Phys. Rev. Appl.* 12.6 (2019): 064053.
<https://doi.org/10.1103/PhysRevApplied.12.064053>.
- [28] A.A.Timopheev, R. Sousa, M. Chshiev, H.T. Nguyen and B. Dieny, "Second order anisotropy contribution in perpendicular magnetic tunnel junctions." *Sci. Rep.* 6.1 (2016): 26877. <https://doi.org/10.1038/srep26877>.
- [29] Hyung Keun Gweon, Hyeon-Jong Park, Kyoung-Whan Kim, Kyung-Jin Lee and Sang Ho Lim, "Intrinsic origin of interfacial second-order magnetic anisotropy in ferromagnet/normal metal heterostructures." , *NPG Asia Mater.* 12.1 (2020): 23.
<https://doi.org/10.1038/s41427-020-0205-z>.

[30] R.L. Novak, F. Garcia, E.R.P. Novais, J.P. Sinnecker, A.P. Guimarães, "Micromagnetic study of skyrmion stability in confined magnetic structures with perpendicular anisotropy." *J. Magn. Magn. Mater.* 451 (2018): 749-760. <https://doi.org/10.1016/j.jmmm.2017.12.004>.

[31] Lan Bo, Rongzhi Zhao, Chenglong Hu, Zhen Shi, Wenchao Chen, Xuefeng Zhang and Mi Yan, "Formation of skyrmion and skyrmionium in confined nanodisk with perpendicular magnetic anisotropy." *J. Phys. D: Appl. Phys.* 53.19 (2020): 195001. <http://dx.doi.org/10.1088/1361-6463/ab6d98>.

Figures

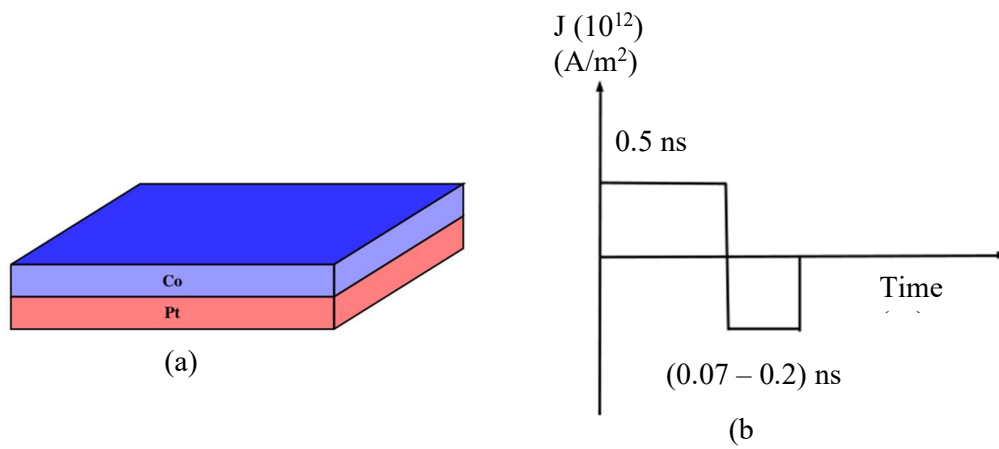


Fig. 1: (a) 200 nm x 200 nm Co/Pt square nano-structure with Co free layer (thickness varied from 1 nm – 5 nm), and (b) Nano-second Current pulse applied to Co/Pt.

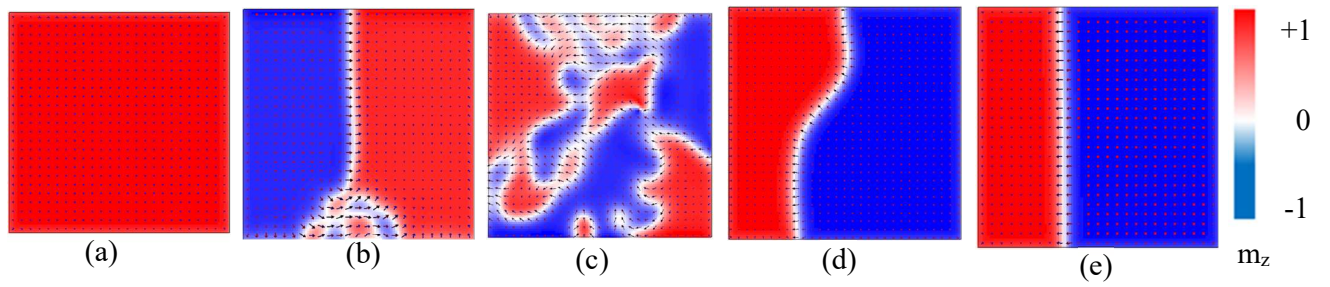


Fig. 2: Magnetization evolution with time for Co layer thickness of 1 nm and applied current density $J = 2 \times 10^{12} \text{ A/m}^2$ in the +z direction for 0.5 ns and in -z direction for 0.1 ns at (a) $t = 0$ s, (b) $t = 0.5$ ns, (c) $t = 0.6$ ns, (d) $t = 1$ ns and (e) $t = 2$ ns.

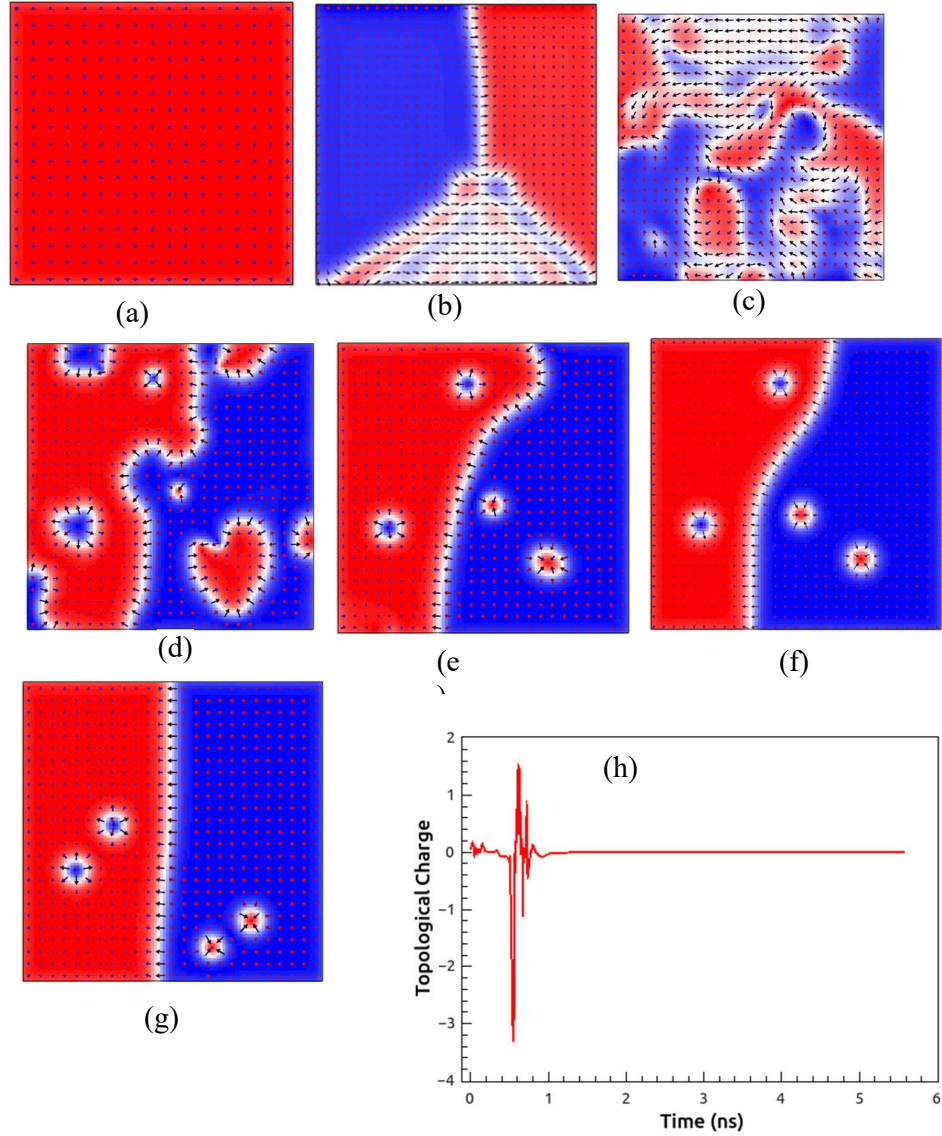


Fig. 3: Spin configurations at (a) $t = 0$ ns, (b) $t = 0.5$ ns, (c) $t = 0.57$ ns, (d) $t = 0.65$ ns, (e) $t = 0.80$ ns, (f) $t = 1$ ns, and (g) $t = 3.75$ ns for $t_{co} = 1$ nm with applied current density $J = 2.3 \times 10^{12}$ A/m² in +z direction for 0.5 ns and in -z direction for 0.07 ns. (h) Topological charge of the sample vs. Simulation time.

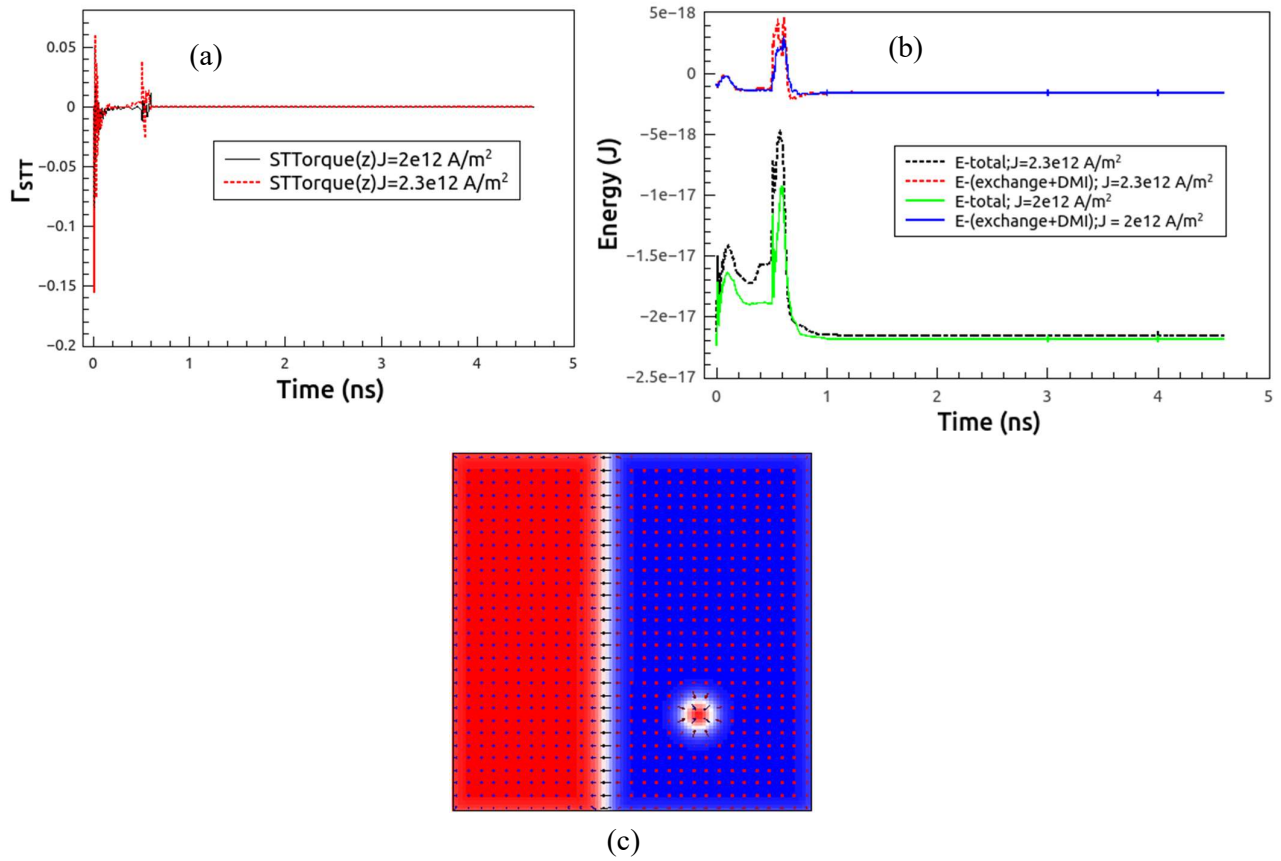


Fig. 4: For a Co free layer thickness of 1 nm (a) Variation of the z component of the STT with simulation time, (b) Energy landscape of the sample for $J = 2 \times 10^{12} \text{ A/m}^2$ and $2.3 \times 10^{12} \text{ A/m}^2$ in +z direction for 0.5 ns and in -z direction for 0.1 ns, and (c) Final relaxed state of the system for $J = 2.3 \times 10^{12} \text{ A/m}^2$.

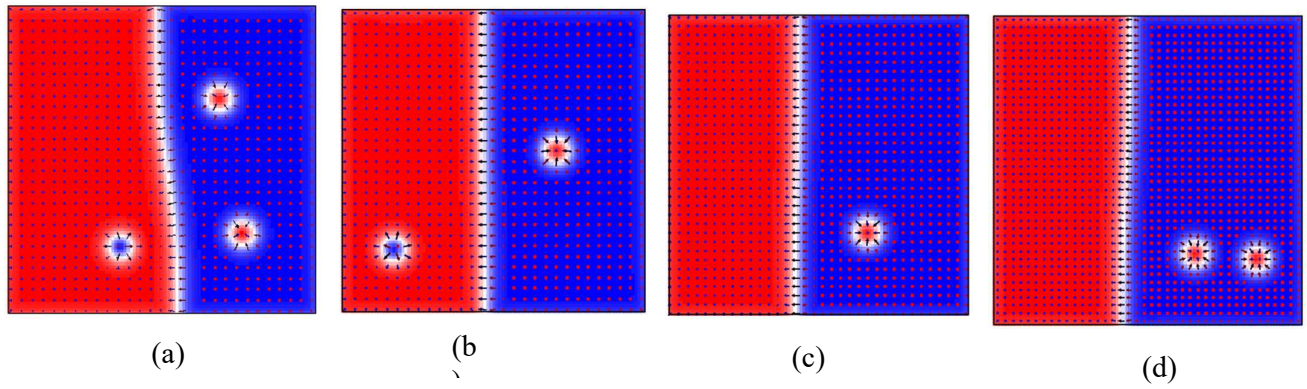


Fig. 5: Stable state of isolated skyrmions for Co layer thickness (a) 2 nm, (b) 3 nm, (c) 4 nm, and (d) 5 nm

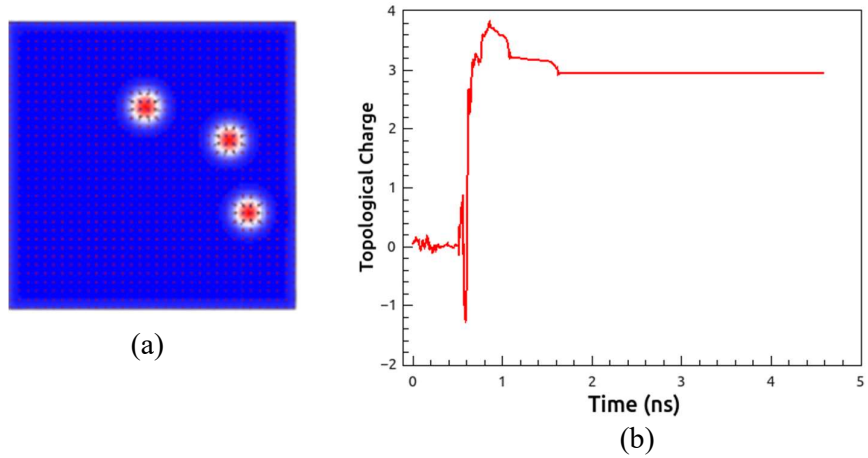


Fig. 6: (a) A stable state of 3 skyrmions is observed for $t_{c_0} = 5$ nm when $J = 10 \times 10^{12}$ A/m² is applied for 0.5 ns in +z direction and for 0.08 ns for in -z direction, and (b) Topological charge vs. simulation time plot, confirms the relaxed state is holding 3 skyrmions of same core magnetization.

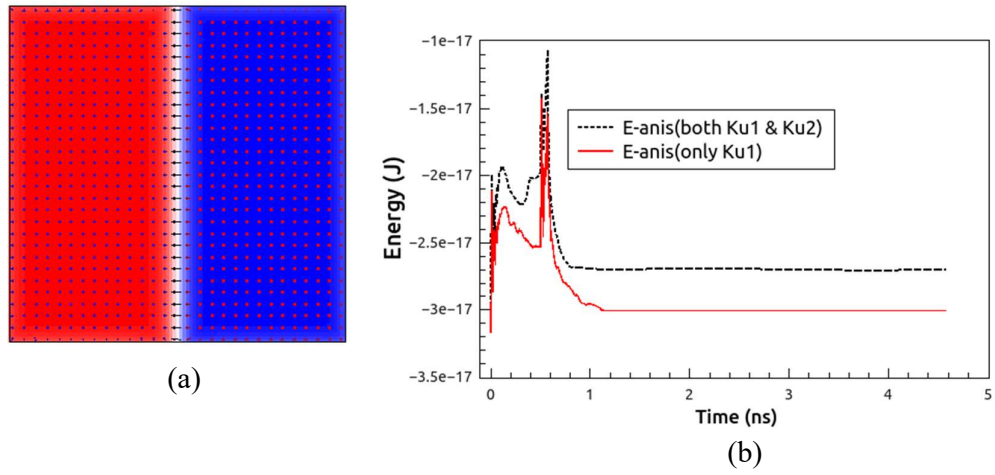


Fig. 7: Final ground state achieved with (a) PMA ($K_{u1} = 8 \times 10^5 \text{ J/m}^3$) for $t_{Co} = 1 \text{ nm}$ and $J = 2.3 \times 10^{12} \text{ A/m}^2$ in $+z$ direction for 0.5 ns and in $-z$ direction for 0.07 ns , and (b) Anisotropy energy comparison plot with time for both the cases.